



Supplementary Information for

Cardiolipin aids in lipopolysaccharide transport to the Gram-negative outer membrane

Martin V. Douglass¹, François Cléon¹ and M. Stephen Trent^{1,2}

¹Department of Infectious Diseases, College of Veterinary Medicine, University of Georgia, Athens GA, 30602

²Department of Microbiology, College of Arts and Sciences, University of Georgia, Athens GA, 30602

Corresponding authors: M. Stephen Trent

Email: strent@uga.edu

This PDF file includes:

Supplemental text
Figures S1 to S10
Tables S1 to S3
SI References

Other supplementary materials for this manuscript include the following:

Dataset S1

Supplementary Materials and Methods.

Efficiency of plating

Bacterial cultures grown overnight were standardized by optical density at 600 nm (OD₆₀₀) and then serially diluted by a factor of 10 in a 96-well plate. Bacteria were transferred to LB plates supplemented with 0.2% glucose using a 96-well plate replicator and grown overnight at 37°C.

Determination of vancomycin minimum inhibitory concentration (MIC)

For a liquid MIC, strains were grown in LB at 37°C at a starting OD₆₀₀ of 0.05 in a range of antibiotic concentrations. The MIC was defined as the lowest antibiotic concentration showing growth <0.05. Additional MICs were determined by E-strip (BioMerieux). Cultures grown to mid-log phase were back diluted and spread on LB plates. A sterile E-strip was added to the dry plate and incubated overnight at 37°C. The MIC was assigned as the value where the zone of inhibition intersected with the E-strip.

DIC microscopy

Bacteria were viewed using a Nikon Instruments Ti Eclipse microscope with A1R scan head (Melville NY). Images were captured in wide field DIC mode with a 488nm laser point scan using a Nikon Plan Apo 60x VC 1.40 oil immersion objective at a resolution of 1024 x 1024 pixels.

Analysis of ³²P-labeled lipid A

Isolation of ³²P-labeled lipid A was carried out as previously described (1, 2). Briefly, cultures were either grown in 2.5 μCi/mL of ³²P ortho-Phosphoric acid (³²P_i) (Perkin-Elmer) to an OD₆₀₀ of 0.8 to 1.0 (Fig 6), or 2.5 μCi/mL of ³²P_i was added to growing cultures at mid-log phase and cells continued to grow for one doubling (Fig 7). Lipid A was extracted via mild-acid hydrolysis followed by Bligh-Dyer solvent extraction as previously described (3). TLC analysis of lipid A samples was done in a pyridine, chloroform, 88% formic acid, aqueous (50:50:16:5 v/v) tank. Plates were exposed to a phosphor screen, imaged, and the percentage of lipid species quantified by densitometry.

GPL radiolabeling

Isolation of ³²P-radiolabeled GPLs was carried out as described previously (4). Briefly, cultures were labeled with 2.5 μCi/mL ³²P_i and grown to an OD₆₀₀ 0.8-1.0, harvested in a clinical centrifuge and washed with PBS. Lipids were extracted by Bligh-Dyer extraction as previously described (2) and TLC carried out using a chloroform, methanol, and acetic acid (65:25:10 vol/vol) solvent system. Plates were exposed to a phosphor screen overnight before imaging.

SDS-PAGE and OmpA Immunoblotting

The OM protein, OmpA, was used as a marker for the OM. Boiled fractions in LDS were loaded in equal volumes (10 μL) from the density gradient and analyzed by SDS-PAGE using a 10% Bis-Tris gel (Fisher). Western blot analysis was carried out via a gel transfer to a low fluorescent polyvinylidene fluoride (PVDF) membrane (Thermo Scientific) using the Novex Xcell II Blot Module. All blots were blocked overnight in a 2% ECL prime blocking agent. The primary rabbit monoclonal α-OmpA (LifeSpan Biosciences) was used at a 1:40000 dilution and a goat anti-rabbit cyanine5 polyclonal served as the secondary antibody (Fisher). Blots were imaged on a Typhoon NIR Plus (Amersham).

NADH Oxidase Assay

The inner membrane enzyme, NADH oxidase, was used as a marker for the IM as previously described (5). Briefly, 2.5 μL of each fraction from the sucrose density gradient was added to a 96-well black bottom plate containing 180 μL of 100 mM Tris HCl, pH 8.0 containing 120 μM NADH (Sigma) and 5 mM dithiothreitol (DTT, Sigma) per well. Changes in fluorescence over time with an excitation at 340 nm and emission at 465 nm was monitored. The activity of NADH oxidase for each fraction is represented as a % of total NADH oxidase activity in the gradient.

Construction of the strain MVD3*clsA* [Δ *clsA*, Δ *lpxM*::kan (pBAD18-*clsA*)] and MVD3*lpxM* [Δ *clsA*, Δ *lpxM*::kan (pBAD18-*lpxM*)]

The Δ *lpxM*::kan allele was transduced using a P1 phage from the Keio collection into W3110 Δ *clsA* pBAD18-*clsA* and W3110 Δ *clsA* pBAD-*lpxM*. Transductants were selected on agar containing kan and 0.2%

L-arabinose. Transductants were confirmed by PCR the using the primers for both *clsA* (using *ClsA_F*: GCGTAAACTCATAACAATGCGCTTTC, *ClsA_R*: GTTTAACCTCTGTTGGCGACGTTTTAC) and *lpxM* (using *LpxM_F*: CCGCTACACTATCACCAGATTG, *LpxM_R*: GAACTTATCATCAGGCGAAGG).

Construction of the strain MVD7 [Δ *clsA*, Δ *lpxM::kan* (pBAD18-*msbA*)]

The Δ *lpxM::kan* allele was transduced using a P1 phage from the Keio collection into W3110 Δ *clsA* pBAD18-*msbA*. Transductants were selected on kan plates containing 0.2% L-arabinose. Transductants were confirmed by PCR using the primers for both *clsA* (using *ClsA_F*: GCGTAAACTCATAACAATGCGCTTTC, *ClsA_R*: GTTTAACCTCTGTTGGCGACGTTTTAC) and *lpxM* (using *LpxM_F*: CCGCTACACTATCACCAGATTG, *LpxM_R*: GAACTTATCATCAGGCGAAGG).

Construction of the strain MVD13 [*yejM569::kan*]

The strain was constructed by λ Red Recombinase as previously described (6). To generate the *yejM569::kan* allele, the kan resistance cassette and FRT sites were amplified from plasmid pKD4 using primers *YejM569_F_Recomb* and *YejM569_R_Recomb*. The *yejM569::kan* DNA was purified and electroporated into strain W3110 pKD46. Recombinants were selected on LB agar containing kan, and the presence of *yejM569::kan* was confirmed by PCR. The kan resistance cassette was removed using pCP20.

Plasmid construction

pBAD18-*clsA*

clsA was amplified from gDNA using primers *ClsA_RBS_xbaI_F* (GATTCTAGATGCGCTTTCAAAAGGATTTTC) and *ClsA_Sall_R* (CTAGTCGACTTACAGCAACGGACTGAAGAAG). The resulting insert was cloned into vector pBAD18 using restriction enzymes *xbaI* and *Sall*.

pBAD-*lpxM*

lpxM was amplified from gDNA using primers *LpxM_RBS_EcoRI_R* (TAAGACGAATTCTGCCTTATCCGAAACTGG) and *LpxM_KpnI_R* (GTCTTAGGTACCCTCTCCTCGCGAGAGGC). The resulting insert was cloned into vector pBAD18 using restriction enzymes *EcoRI* and *KpnI*.

pBAD-*msbA*

msbA was amplified from gDNA using primers *MsbA_RBS_BamHI_F* (TAAGACGGATCCATAACGGGTAGAATATGCGGC) and *MsbA_HindIII_R* (GTCTTAAAGCTTACCAGACCAGATTTTTTCG). The resulting insert was cloned into vector pBAD18 using restriction enzymes *BamHI* and *HindIII*.

pBAD-*clsB*

clsB was amplified from gDNA using primers *ClsB_RBS_EcoRI_F* (TAAGACGAATTCATGCCCTTTAAGTGCGG) and *ClsB_KpnI_R* (GTCTTAGGTACC~~CGCGGGTGTGATTTACTCATCAGG~~). The resulting insert was cloned into vector pBAD18 using restriction enzymes *EcoRI* and *KpnI*.

pBAD18-*ymdB-clsB*

ymdB and *clsC* were amplified in tandem from gDNA using primers *YmdB_RBS_EcoRI_F* (TAAGACGAATTC~~CAAGAAGGTGTAAGGAGGC~~) and *ClsC_KpnI_R* (GTCTTAGGTACCAGCACCAGCCCGTTAAGC). The resulting insert was cloned into vector pBAD18 using restriction enzymes *EcoRI* and *KpnI*.

pACYC184-*lpxE*

lpxE was amplified from gDNA of *Francisella novicida* U112 using primers *LpxE_RBS_BamHI_F* (TAAGACGGATCCGCTTGTA~~ACTATCTAATTAATAGG~~) and *LpxE_Sall_R* (GTCTTAGT~~CGACTAGTAATATTTACAATAGC~~). The resulting insert was cloned into vector pBAD18 using restriction enzymes *BamHI* and *Sall*.

pBAD18-*clsA*_{H224A}

Site directed mutagenesis was performed on pBAD18-*clsA* using Agilent QuikChange II kit, following manufactures instructions. Primers *ClsA*_H224A_F (TGATCATCTTGCGAGCTTGGCGCAGGTCCATACGG) and *ClsA*_H224A_R (CCGTATGGACCTGCGCCAAGCTCGCAAGATGATCA) were used.

pCV3-*clsA*_{H224A}

*clsA*_{H224A} was amplified from pBAD-*clsA*_{H224A} using primers *ClsA*_BspQI_F (NNGCTCTTCNTTCATGACAACCGTTTATA) and *ClsA*_BspQI_R (NNGCTCTTCNTTATTACAGCAACGGACTG). The resulting insert was cloned into vector pCV3 using the restriction enzymes BspQI.

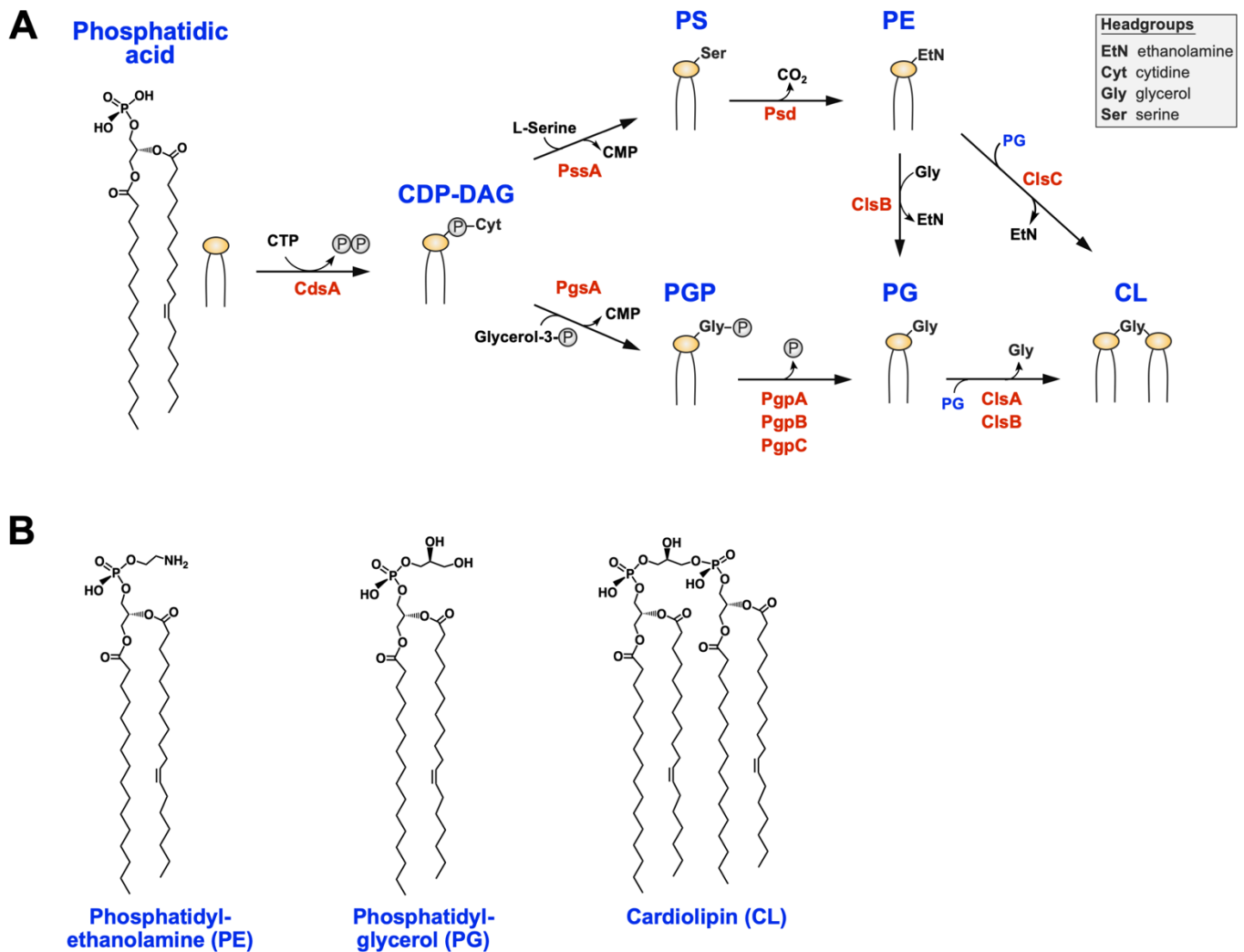


Fig. S1. Pathway pathway for glycerophospholipid (GPL) biosynthesis and structures of the major GPLs in *E. coli*. **A.** Phosphatidic acid, that is generated at the cytoplasmic surface of the IM, is activated using cytidine nucleotides allowing for subsequent phosphatidyl-transfer reactions. CdsA (CDP-DAG synthase) converts phosphatidic acid to cytidine diphosphate diacylglycerol using cytidine triphosphate (CTP). CDP-DAG then functions as a donor of phosphatidyl moieties to generate phosphatidylserine (PS) by phosphatidylserine synthase (PssA) and phosphatidylglycerol-3-phosphate (PGP) by phosphatidylglycerol phosphate synthase (PgsA). PS is quickly decarboxylated by the enzyme Psd yielding the bulk GPL in *E. coli*, phosphatidylethanolamine (PE). An inner membrane phosphatase (either PgpA, PgpB, or PgpC) dephosphorylates PGP to yield phosphatidylglycerol (PG) which is the second most abundant GPL in *E. coli*. Finally, cardiolipin (CL) arises from the condensation of two PG molecules by either ClsA or ClsB. ClsC, however, utilizes PE and PG to form CL. Enzyme names are in red, major substrates are in blue, and cofactors in black. **B.** Chemical structures of the major glycerophospholipids.

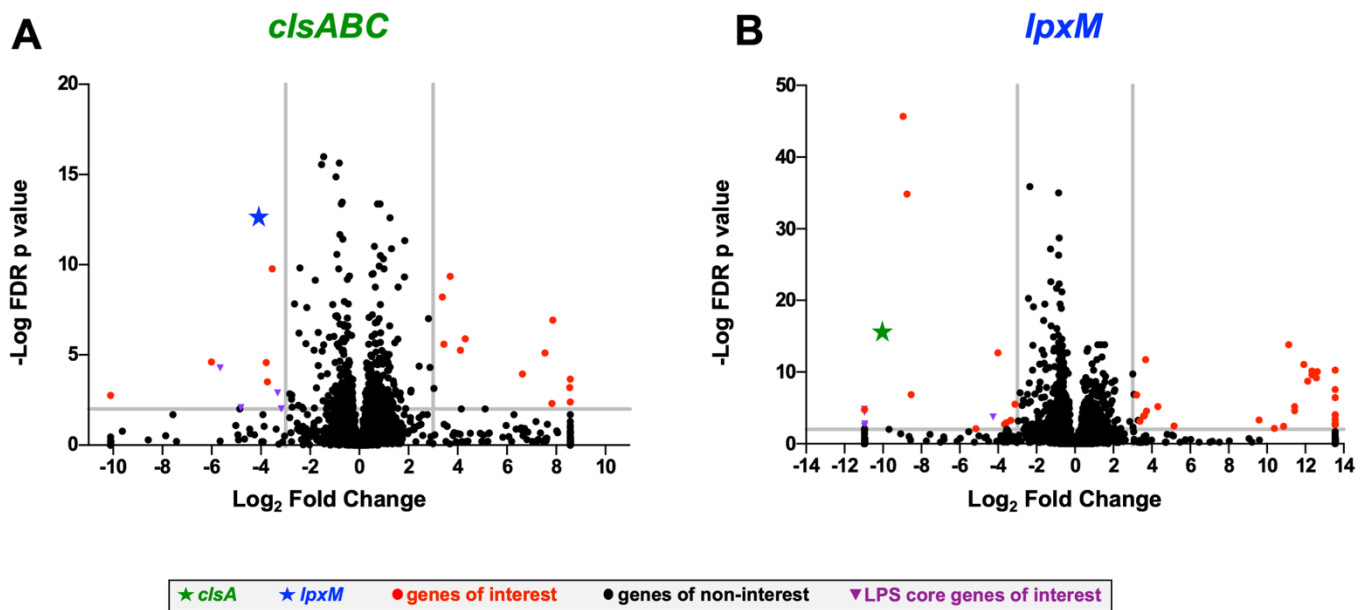


Fig. S2. Volcano plot of genes revealed by Tn-seq analysis. Genes of interest were highlighted (red) that have a cut-off of \log_2 fold change >3 or <-3 (vertical grey lines), and a False Discovery Rate (FDR) p value <0.05 (horizontal grey line) in a genetic background of $\Delta clsABC$ (**A**) or $\Delta lpxM$ (**B**). For a more complete visual representation, in **A** genes *yrbC*, *cpxR*, *nlpI*, *rfaQ*, *yrbD*, *vacJ*, *argB* and in **B** gene *tolC* are not shown. These genes were under the fold change cut off but expressed a high FDR p value.

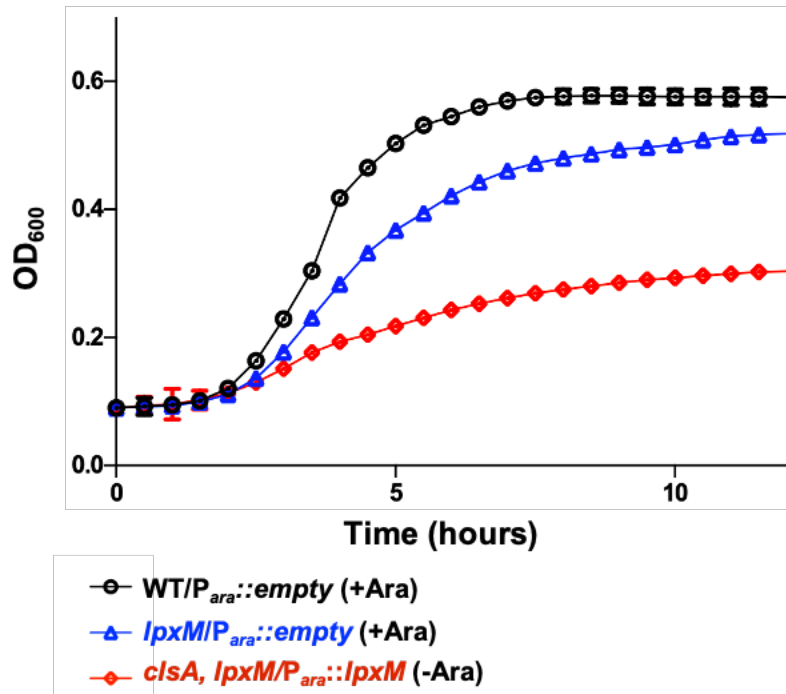


Fig. S3. Depletion of LpxM in the absence of ClsA leads to a growth defect. Cells of *clsA*, *lpxM*/*P_{ara}::lpxM* were grown under repressing conditions with 0.2% glucose (red) (-Ara). WT cells were used as a control. Growth of indicated strains were monitored by OD₆₀₀ every 30 minutes. Error bars represent SEM from technical triplicate.

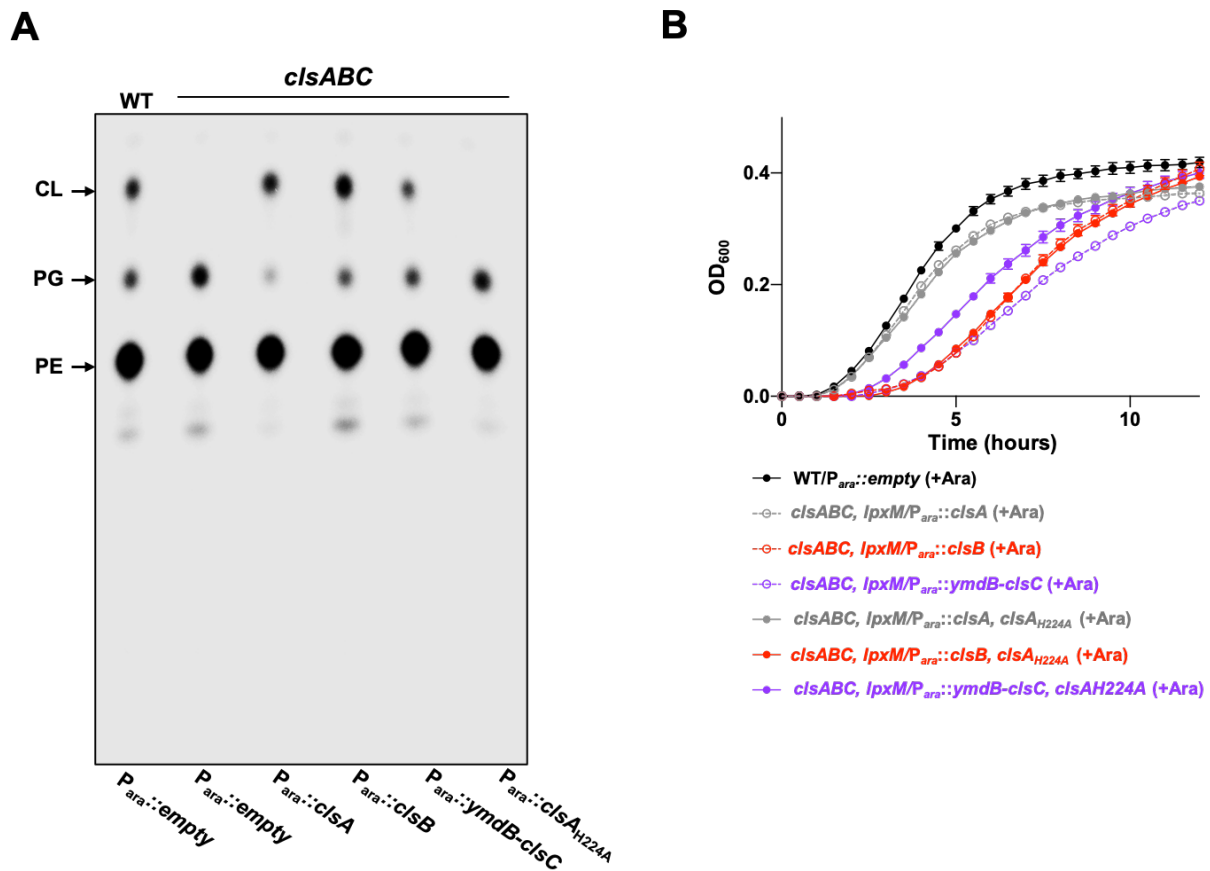


Fig. S4. Cardiolipin synthesized by CIsB or CIsC cannot fully rescue the *clsA*, *lpxM* synthetic phenotype. **A.** Cardiolipin synthesized by different CIs enzymes. CL deficient Δ *clsABC* mutants harboring different *cls* genes down stream of an inducible promoter were grown in the presence of 0.2% arabinose to induce *cls* expression. Cells were grown to an OD₆₀₀ ~1.0 in the presence of ³²P_i in LB media. Extracted GPLs were separated by TLC and visualized by phosphorimaging. The positions of PE, PG, and CL are indicated, and the TLC is representative of 2 biological experiments. **B.** Growth Curve of CL deficient *lpxM* mutants expressing individual CIs enzymes. Cells were grown in inducing conditions in 0.2% arabinose and growth of indicated strains were monitored by OD₆₀₀ every 30 minutes. Error bars represent SEM from technical triplicate.

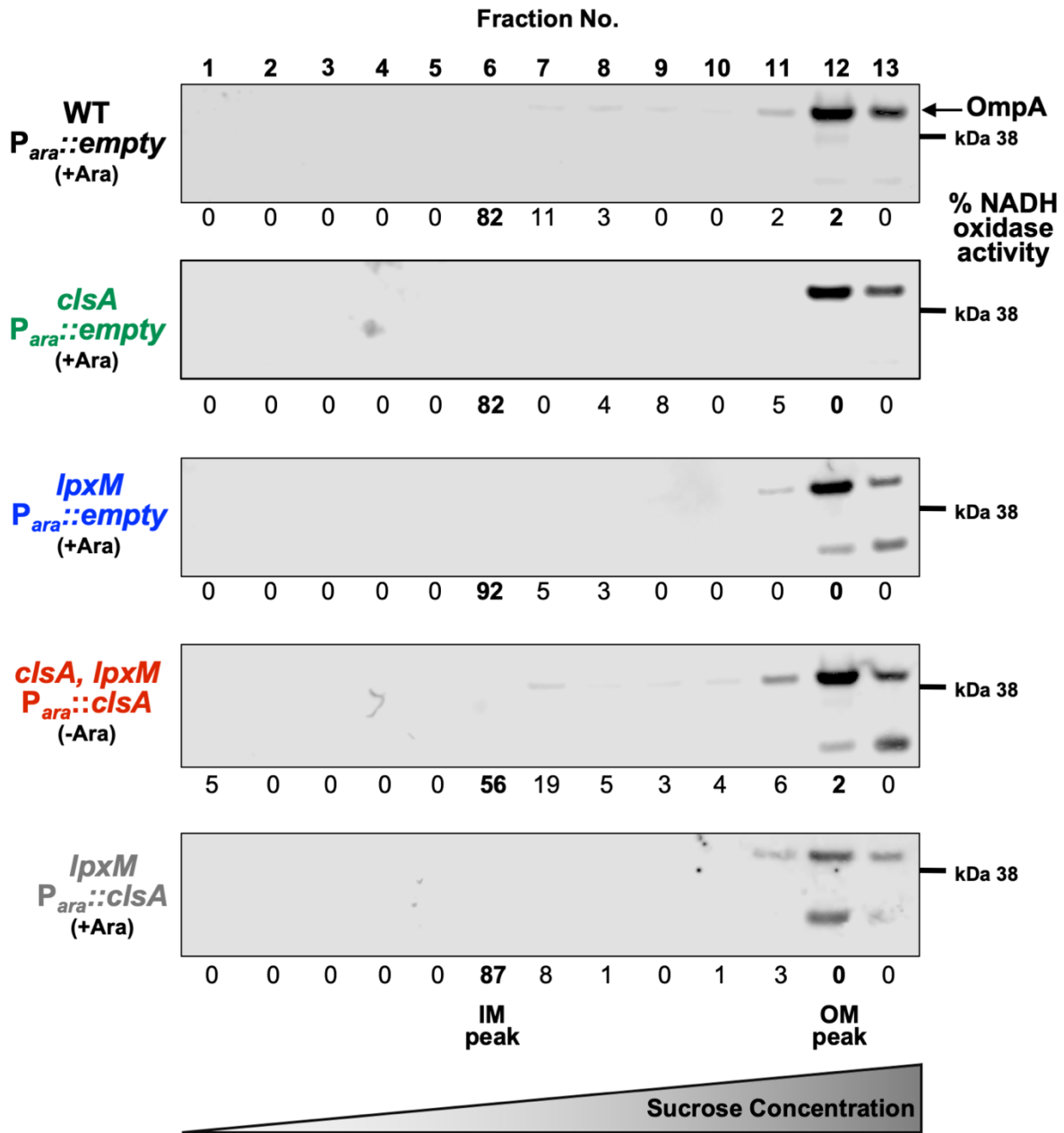


Fig. S5. Analysis of NADH oxidase activity (IM marker) and presence of OmpA (OM marker) of sucrose gradient fractions. Fractions from Fig 4. were analyzed by SDS-PAGE and Western blot for the presence of the OM β -barrel OmpA using α -OmpA antibody. NADH oxidase activity was measured for each fraction as previously described (1) and the % activity of each fraction across the gradient has been indicated.

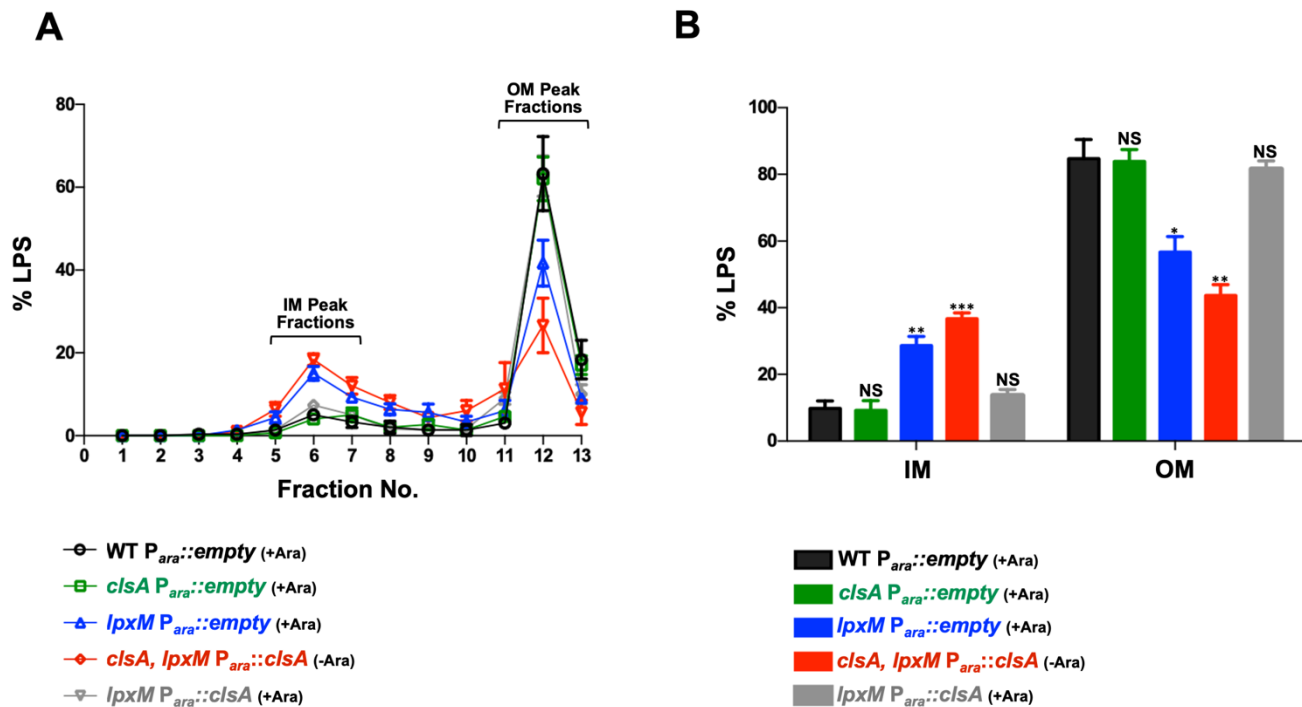


Fig. S6. LPS quantification across inner and outer membrane fractions. **A.** LPS Density across membrane separation gradient. % LPS density was analyzed in biological triplicate as shown in **Fig. 5**. **B.** Inner membrane (IM) and outer membrane (OM) % LPS. Pooled membrane LPS levels were determined by adding the % LPS from the expected membrane fraction locations as seen in **Fig. S5**. With the inner membrane located between fractions 5-7, and the outer membrane located between fractions 11-13. Error bars represent SEM from biological triplicate. T-test used between strains. $0.05 > P^*$, $0.01 > P^{**}$, $0.001 > P^{***}$.

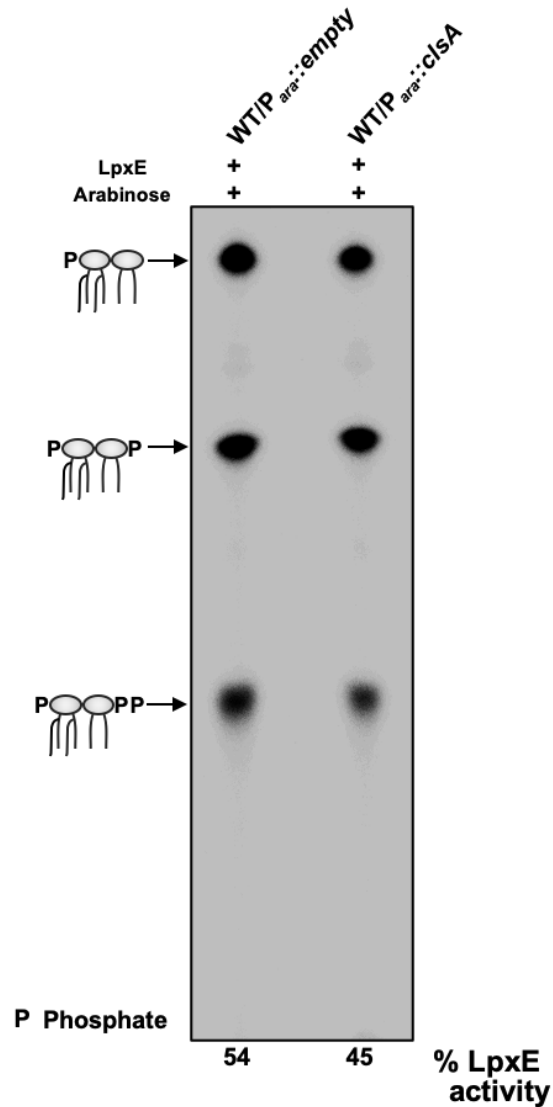


Fig. S7. Over expression of ClsA does not increase LpxE activity in a wild type background. Indicated strains were grown in the presence 0.2% arabinose to induce plasmid expression. Cultures were grown to mid-log phase and then inoculated with $^{32}\text{P}_i$ and grown for one doubling phase. Lipid A was isolated, separated by TLC and visualized by phosphorimaging. % LpxE is calculated by densitometry of the mono-phosphate lipid A divided by total densitometry. Lipid A species are listed. The TLC is representative of 3 biological triplicates.

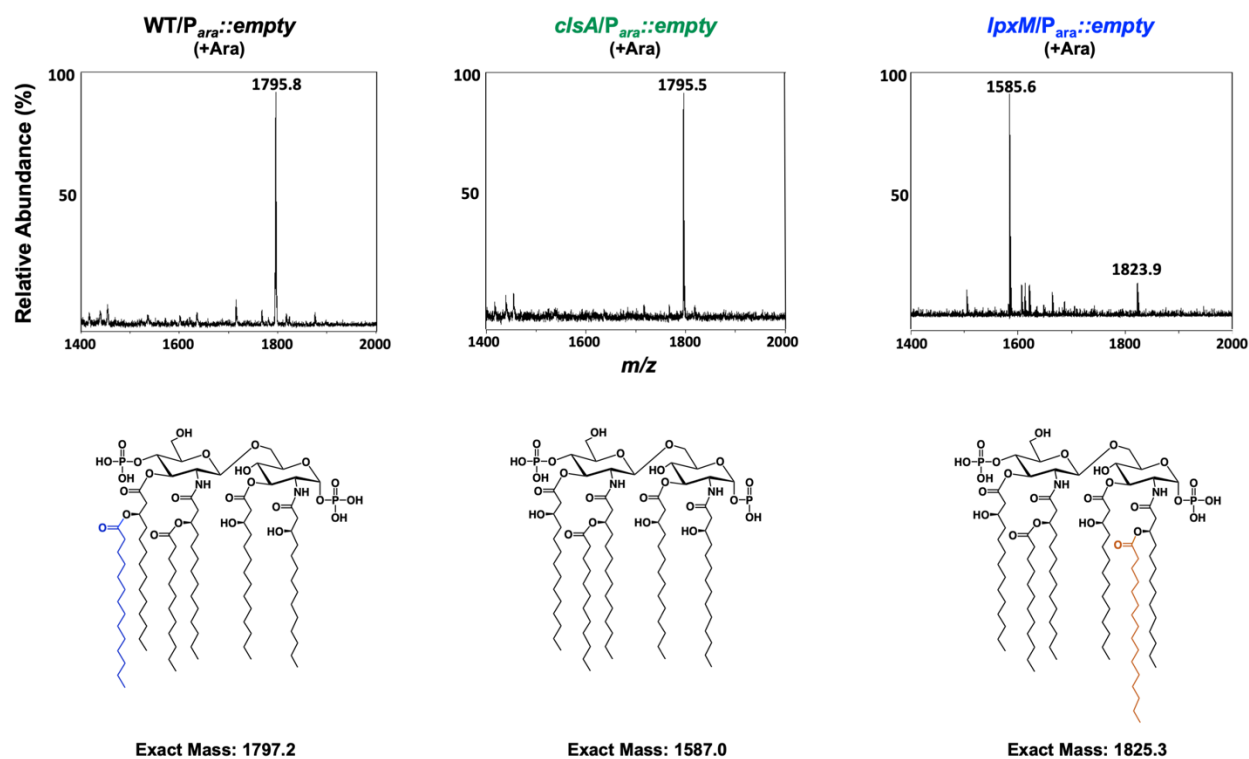


Fig. S8. MALDI-TOF mass spectrometry of lipid A. The lipid A of the indicated strains were purified as previously described (7) and analyzed by MALDI-TOF mass spectrometry. 5-Chloro-2-mercaptobenzothiazole was used as the matrix. Lipid A structures and their corresponding exact masses are provided for reference. WT and *clsA* show prominent spectral peaks at *m/z* 1795.8 and 1795.5, respectively. These peaks correspond to the major bis-phosphorylated, hexa-acylated lipid A of *E. coli* K-12. Absence of *lpxM* results in a major peak with an *m/z* of 1585.6 corresponding to penta-acylated lipid A and an additional peak at *m/z* 1822.9 corresponding to the addition of palmitate (C16:0) by the outer membrane enzyme PagP. **Note:** The tris-phosphorylated lipid A species containing a diphosphate at the 1-position is not detected using this particular matrix and instrument (see Fig. 6).

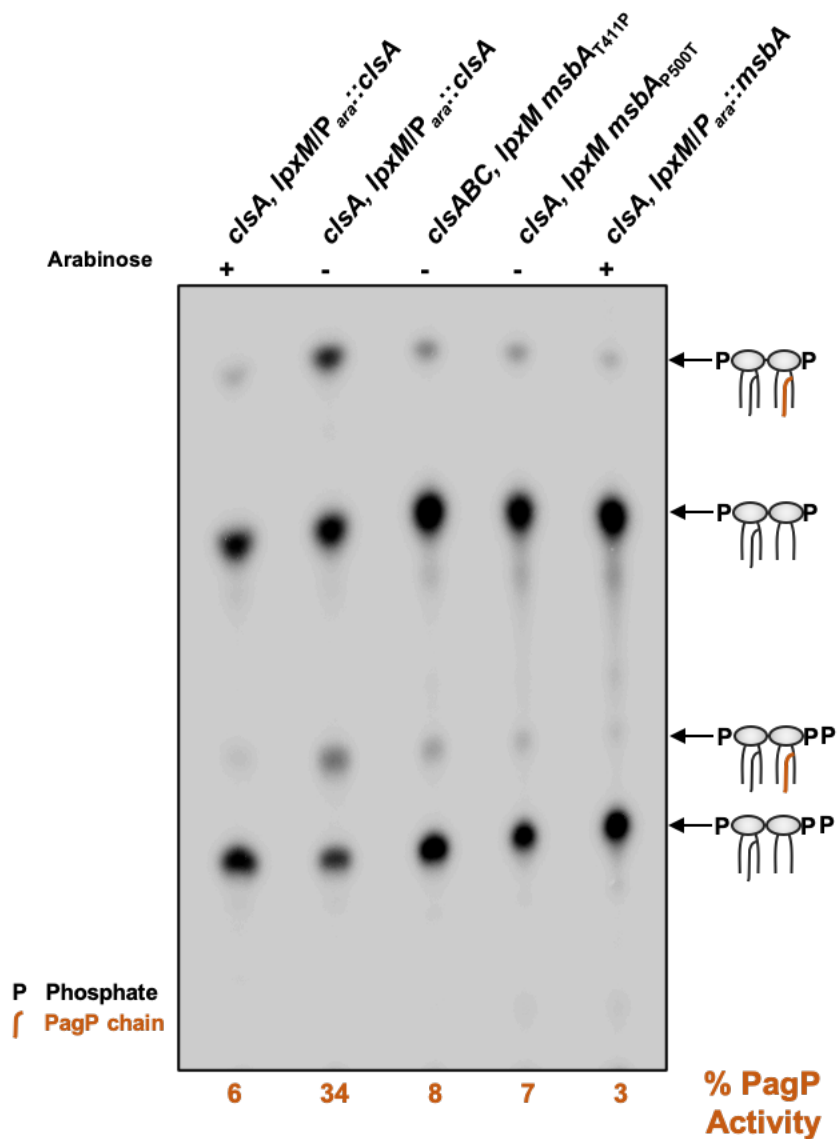


Fig. S9. *msbA* suppressors have decreased levels of PagP modified lipid A. Indicated strains were grown in the presence 0.2% arabinose to induce plasmid expression, or in 0.2% glucose to repress plasmid expression, cultures were grown to mid-log phase in the presence of $^{32}\text{P}_i$. Lipid A was isolated, separated by TLC and visualized by phosphorimaging. PagP modified lipid A was measured as percent of total densitometry. Lipid A species are indicated.

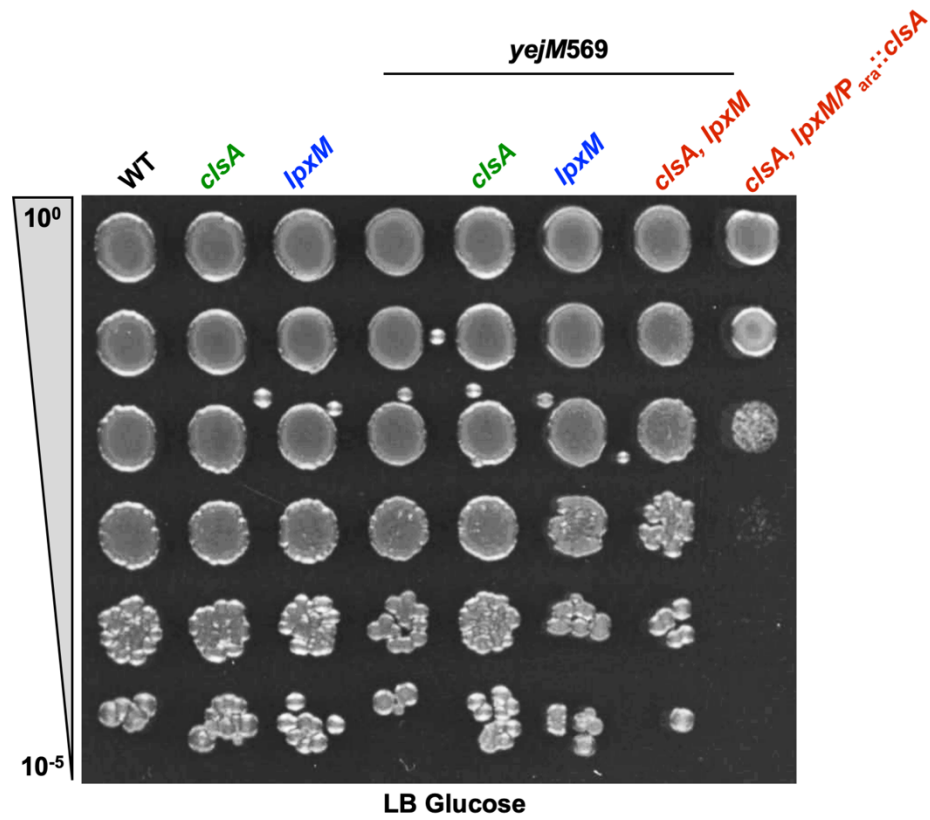


Fig. S10. Efficiency of plating for *yejM569* mutant strains. Serial dilutions of the indicated strains were spotted on LB plates containing 0.2% glucose and grown overnight at 37°C.

Table S1. Vancomycin MICs of various strains.

Strain	Vancomycin MIC ($\mu\text{g/mL}$)*
WT/ <i>P_{ara}::empty</i> (+Ara)	>256
<i>lpxM</i> / <i>P_{ara}::empty</i> (+Ara)	48
<i>lpxM</i> / <i>P_{ara}::clsA</i> (+Ara)	128
<i>lpxM</i> / <i>P_{ara}::lpxM</i> (+Ara)	>256
MG1655	>256
MG1655 <i>lpxM</i> / <i>P_{ara}::empty</i> (+Ara)	128
MG1655 <i>lpxM</i> / <i>P_{ara}::clsA</i> (+Ara)	256
MG1655 <i>lpxM</i> / <i>P_{ara}::lpxM</i> (+Ara)	>256
W3110	>256
<i>fabR</i>	256
Δ <i>clsABC</i>	192
<i>clsABC, fabR</i>	128
<i>lpxM</i>	48
<i>lpxM, fabR</i>	32
<i>clsABC, fabR, lpxM</i>	32
<i>clsABC, lpxM fabF_{T196M}</i>	32
<i>clsABC, lpxM msbA_{T411P}</i>	96
<i>clsA, lpxM msbA_{P500T}</i>	96
<i>clsA, lpxM</i> / <i>P_{ara}::msbA</i>	64
<i>clsA, lpxM, yejM569</i>	48

*Vancomycin MIC was measured by E-test. Cultures were grown overnight in LB. Overnight cultures were back diluted 1:100 in LB with or without 0.2% arabinose. Cultures grown until OD₆₀₀ 0.5 reached. Diluted cells were then spread across LB plates with or without 0.2% arabinose. An E-test was placed on lawn and incubated overnight at 37 °C. MIC was determined by visualizing a clear zone of inhibition.

Table S2: Strains and plasmids used in this study

Strain	Description	Source or reference
<i>E. coli</i> W3110	Wild type, F- λ -, <i>rphH-1 IN(rrnD, rrnE)</i> 1	<i>E. coli</i> Genetic Stock Center (Yale)
BKT10a	W3110 Δ <i>clsA</i>	(8)
BKT11a	W3110 Δ <i>clsA</i> , Δ <i>clsB</i>	(6)
BKT12	W3110 Δ <i>clsA</i> , Δ <i>clsB</i> , Δ <i>clsC::kan</i>	(8)
BKT12a	W3110 Δ <i>clsA</i> , Δ <i>clsB</i> , Δ <i>clsC</i> , derived from BKT12	This study
BKT13	W3110 Δ <i>clsB::kan</i>	(8)
BK13a	W3110 Δ <i>clsB</i> , derived from BKT13	This study
BKT14a	W3110 Δ <i>clsC</i>	(8)
BKT15	W3110 Δ <i>clsA</i> , Δ <i>clsC::kan</i>	(8)
BKT15a	W3110 Δ <i>clsA</i> , Δ <i>clsC</i> , derived from BKT15	This study
BKT16	W3110, Δ <i>clsB::kan</i> , Δ <i>clsC</i>	(8)
BKT16a	W3110, Δ <i>clsB</i> , Δ <i>clsC</i> , derived from BKT16	This study
MVD1	W3110, Δ <i>lpxM</i>	This study
MVD3 <i>clsA</i>	W3110, Δ <i>clsA</i> , Δ <i>lpxM::kan</i> (pBAD18- <i>clsA</i>), derived from BKT10a	This study
MVD3 <i>lpxM</i>	W3110, Δ <i>clsA</i> , Δ <i>lpxM::kan</i> (pBAD18- <i>lpxM</i>), derived from BKT10a	This study
MVD15	W3110, Δ <i>clsABC</i> , (pBAD18- <i>clsA</i>), derived from BKT12a	This study
MVD16	W3110, Δ <i>clsABC</i> , (pBAD18- <i>clsB</i>), derived from BKT12a	This study
MVD17	W3110, Δ <i>clsABC</i> , (pBAD18- <i>ymdB-clsC</i>), derived from BKT12a	This study
MVD18	W3110, Δ <i>clsABC</i> , (pBAD18- <i>clsA_{H224A}</i>), derived from BKT12a	This study
MVD19	W3110, Δ <i>clsABC</i> , Δ <i>lpxM::kan</i> (pBAD18- <i>clsA</i>), derived from MVD15	This study
MVD20	W3110, Δ <i>clsABC</i> , Δ <i>lpxM::kan</i> (pBAD18- <i>clsB</i>), derived from MVD16	This study
MVD21	W3110, Δ <i>clsABC</i> , Δ <i>lpxM::kan</i> (pBAD18- <i>ymdB-clsC</i>), derived from MVD17	This study
MVD22	W3110, Δ <i>clsABC</i> , Δ <i>lpxM::kan</i> (pBAD18- <i>clsA</i> , pCV3- <i>clsA_{H224A}</i>), derived from MVD19	This study
MVD23	W3110, Δ <i>clsABC</i> , Δ <i>lpxM::kan</i> (pBAD18- <i>clsB</i> , pCV3- <i>clsA_{H224A}</i>), derived from MVD20	This study
MVD24	W3110, Δ <i>clsABC</i> , Δ <i>lpxM::kan</i> (pBAD18- <i>ymdB-clsC</i> , pCV3- <i>clsA_{H224A}</i>), derived from MVD21	This study
MG1655	F- λ -, <i>rph-1</i>	<i>E. coli</i> Genetic Stock Center (Yale)
MVD4	MG1655, Δ <i>lpxM</i>	This study

MVD5	W3110, Δ <i>clsABC</i> , Δ <i>lpxM::kan</i> , <i>msbA(T411P)</i> , derived from BKT12a	This study
MVD6	W3110, Δ <i>clsA</i> , Δ <i>lpxM::kan</i> , <i>msbA(P500T)</i> , derived from BKT10a	This study
MVD7	W3110, Δ <i>clsA</i> , Δ <i>lpxM::kan</i> (pBAD18- <i>msbA</i>), derived from BKT10a	This study
MVD8 <i>clsA</i>	W3110, Δ <i>lpxM</i> +(pBAD- <i>clsA</i>), derived from MVD1	This study
MVD9	W3110, Δ <i>clsABC</i> , Δ <i>lpxM::kan</i> , <i>fabF(T196M)</i> , derived from BKT12a	This study
MVD10	W3110, Δ <i>clsABC</i> , Δ <i>fabR</i> , Δ <i>lpxM::kan</i> , derived from BKT12a	This study
MVD11	W3110, Δ <i>clsABC</i> , Δ <i>fabR::kan</i> , derived from BKT12a	This study
MVD12	W3110, Δ <i>lpxM</i> , Δ <i>fabR::kan</i> , derived from MVD1	This study
MVD13	W3110, <i>yejM569::kan</i>	This study
MVD14	W3110, Δ <i>clsA</i> , <i>yejM569</i> , Δ <i>lpxM::kan</i> , derived from MVD13	This study
Plasmid	Description	Source or reference
pCP20	FLP recombinase expression; Amp ^R CamR; temperature-sensitive replicon	(9)
pKD4	Plasmid containing a kan resistance cassette flanked by FRT sites	(6)
pKD46	Plasmid which encodes a λ Red Recombinase system from temperature sensitive promoter	(6)
pBAD18	High copy expression plasmid, Amp ^R , <i>P_{ara}:: empty</i> , PBR322 origin	(10)
pBAD18- <i>clsA</i>	Amp ^R , <i>P_{ara}::nativeRBS clsA</i>	This study
pBAD18- <i>lpxM</i>	Amp ^R , <i>P_{ara}::nativeRBS lpxM</i>	This study
pBAD18- <i>clsB</i>	Amp ^R , <i>P_{ara}::nativeRBS clsB</i>	This study
pBAD18- <i>ymdB-clsC</i>	Amp ^R , <i>P_{ara}::nativeRBS_ymdB-clsC</i> , cloned in tandem	This study
pBAD18- <i>clsA_{H224A}</i>	Amp ^R , <i>P_{ara}::nativeRBS clsA</i> , with H224A substitution	This study
pBAD18- <i>msbA</i>	Amp ^R , <i>P_{ara}::nativeRBS msbA</i>	This study
pCV3	Cam ^R , p15A origin	(11)
pCV3- <i>clsA_{H224A}</i>	Cam ^R , <i>P_{ara}::clsA_{H224A}</i>	This study
pACYC184	Tet ^R , CamR, PSC101 p15A origin	Novagen
pACYC184- <i>lpxE</i>	<i>lpxE</i> cloned into pACYC184	This study

Table. S3: Primers used in this study

Primer name	DNA sequence (5'-3')*	Strain or plasmid
ClsA_F	GCGTAAACTCATAACAATGCGCTTTC	BKT10a
ClsA_R	GTTTAACCTCTGTTGGCGACGTTTTAC	BKT10a
ClsA_RBS_xbaI_F	GATTCTAGATGCGCTTTCAAAGGATTC	pBAD18- <i>clsA</i> MVD3C
ClsA_Sall_R	CTAGTCGACTTACAGCAACGGACTGAAGAAG	pBAD18- <i>clsA</i> MVD3C
ClsA_H224A_F	TGATCATCTTGCGAGCTTGGCGCAGGTCCATACGG	pBAD18- <i>clsA</i> _{H224A}
ClsA_H224A_R	CCGTATGGACCTGCGCCAAGCTCGCAAGATGATCA	pBAD18- <i>clsA</i> _{H224A}
LpxM_F	CCGCTACACTATCACCAGATTG	MVD1
LpxM_R	GAAGTTATCATCAGGCGAAGG	MVD1
LpxM_RBS_EcoRI_R	TAAGACGAATTCTGCCTTATCCGAAACTGG	pBAD18- <i>lpxM</i> MVD3L
LpxM_KpnI_R	GTCTTAGGTACCCTCTCCTCGCGAGAGGC	pBAD18- <i>lpxM</i> MVD3L,
MsbA_RBS_BamHI_F	TAAGACGGATCCATAACGGGTAGAATATGCGGC	pBAD18- <i>msbA</i> MVD7
MsbA_HindIII_R	GTCTTAAAGCTTCACCAGACCAGATTTTTTCG	pBAD18- <i>msbA</i> MVD7
LpxE_RBS_BamHI_F	TAAGACGGATCCGCTTGTAACTATCTAATTAATAGG	pACYC184- <i>lpxE</i>
LpxE_Sall_R	GTCTTAGTTCGACTAGTAATATTTACAATAGC	pACYC184- <i>lpxE</i>
ClsB_RBS_EcoRI_F	TAAGAC GAATTCATGCCCT TTAAGTGCGG	pBAD18- <i>clsB</i>
ClsB_KpnI_R	GTCTTAGGTACC GCGCGGGTGTGATTTACTCATCAGG	pBAD18- <i>clsB</i>
YmdB_RBS_EcoRI_F	TAAGACGAATTCCAAGAAGGTGTAAGGAGGC	pBAD18- <i>ymdB-clsC</i>
ClsC_KpnI_R	GTCTTAGGTACCAGCACCAGCCCGTTAAGC	pBAD18- <i>ymdB-clsC</i>
ClsA_BspQI_F	NNGCTCTTCNTTCATGACAACCGTTTATA	pCV3- <i>clsA</i> _{H224A}
ClsA_BspQI_R	NNGCTCTTCNTTATTACAGCAACGGACTG	pCV3- <i>clsA</i> _{H224A}
YejM569_F_R ecomb	ATTCTTATTTATCGCCTTTATCGCCTCGCATGTGGTGTATATCTGAGTGTAGGCTGGAGCTGCTTC	MVD13
YejM569_R_R ecomb	GGACCATGGCTAATTCCCATTTAATTATAAATCAGTTAGCGAAATATCTTACTTGCAATCGGTGT	MVD13
YejM569_F	CCTCGCATGTGGTGTATATC	MVD13
YejM569_R	CTTACTTGCAATCGGTGTGG	MVD13

*Underlined sequences denote restriction enzyme cut sites

Dataset S1 (separate file). Tn-Seq analysis of *cls* and *lpxM* mutants.

Supplementary information references

1. B. Ma, C. M. Reynolds, C. R. H. Raetz, Periplasmic orientation of nascent lipid A in the inner membrane of an Escherichia coli LptA mutant. *PNAS* **105**, 13823–13828 (2008).
2. E. G. Bligh, W. J. Dyer, A rapid method of total lipid extraction and purification. *Can J Biochem Physiol* **37**, 911–917 (1959).
3. S. M. Zimmerman, A.-A. J. Lafontaine, C. M. Herrera, A. B. Mclean, M. S. Trent, A Whole-Cell Screen Identifies Small Bioactives That Synergize with Polymyxin and Exhibit Antimicrobial Activities against Multidrug-Resistant Bacteria. *Antimicrobial Agents and Chemotherapy* **64** (2020).
4. D. Giles, J. Hankins, Z. Guan, M. Trent, Remodeling of the Vibrio cholerae membrane by incorporation of exogenous fatty acids from host and aquatic environments. *Molecular microbiology* **79**, 716–28 (2011).
5. R. Shrivastava, X. Jiang, S.-S. Chng, Outer membrane lipid homeostasis via retrograde phospholipid transport in Escherichia coli. *Molecular Microbiology* **106**, 395–408 (2017).
6. K. A. Datsenko, B. L. Wanner, One-step inactivation of chromosomal genes in Escherichia coli K-12 using PCR products. *Proc. Natl. Acad. Sci. U.S.A.* **97**, 6640–6645 (2000).
7. C. M. Herrera, J. C. Henderson, A. A. Crofts, M. S. Trent, Novel coordination of lipopolysaccharide modifications in Vibrio cholerae promotes CAMP resistance. *Mol. Microbiol.* **106**, 582–596 (2017).
8. B. K. Tan, *et al.*, Discovery of a cardiolipin synthase utilizing phosphatidylethanolamine and phosphatidylglycerol as substrates. *Proc Natl Acad Sci U S A* **109**, 16504–16509 (2012).
9. P. P. Cherepanov, W. Wackernagel, Gene disruption in Escherichia coli: TcR and KmR cassettes with the option of FIp-catalyzed excision of the antibiotic-resistance determinant. *Gene* **158**, 9–14 (1995).
10. L. M. Guzman, D. Belin, M. J. Carson, J. Beckwith, Tight regulation, modulation, and high-level expression by vectors containing the arabinose PBAD promoter. *Journal of bacteriology* **177**, 4121–4130 (1995).
11. C. M. VanDrisse, J. C. Escalante-Semerena, New high-cloning-efficiency vectors for complementation studies and recombinant protein overproduction in Escherichia coli and Salmonella enterica. *Plasmid* **86**, 1–6 (2016).